05,08

Neutron waveguides with magnetic layers

© S.V. Kozhevnikov[1], Yu.N. Khaydukov[2,3,4]

[1] Joint Institute for Nuclear Research, Moscow oblast, Dubna, Russia
[2] Moscow State University, Moscow, Russia
[3] Max Planck Institut für Festkörperforschung, Stuttgart, Germany
[4] Max Planck Society Outstation at FRM-II, Garching, Germany

E-mail: kozhevn@nf.jinr.ru

Received April 18, 2024
Revised April 18, 2024
Accepted May 8, 2024

Tri-layer neutron waveguides with external magnetic layers are considered. In such waveguides it is possible to control the coefficient of enhancement of neutron density by switching the external layers magnetization by the applied magnetic field. In this work, the intensity of the narrow neutron microbeam escaped from the end face of the middle nonmagnetic layer is registered. It is obtained that the intensity of the divergent microbeam depends on the polarization sign of the polarized collimated neutron beam entered on the waveguide surface.

Keywords: polarized neutrons, layered nanostructures, neutron waveguides, neutron resonators.

DOI: 10.61011/PSS.2024.06.58700.14HH

1. Introduction

Neutron scattering is a powerful method for studying polymers, biological objects and magnetic structures owing to the special properties of neutrons: high penetrating power, isotopic sensitivity and the presence of its own magnetic moment. X-ray radiation has a low penetrating power, so it cannot be used to study magnetism in the volume of matter or at a depth from the surface. Polarized neutron beams are a unique tool for such case. The scale of the studied objects is determined by the beam width, which ranges from 0.1 to 10 mm in a conventional neutron experiment. It is necessary to have beams with a width of less than $100\,\mu$m to study local microstructures. Various focusing devices are developed for such purpose (bent crystal-monochromator, refractive lenses, parabolic mirror neutron guides, etc.) [1], which can compress a neutron beam to $50\,\mu$m. Smaller beam sizes cannot be obtained because of limitations that are determined by the physical properties of the materials used or their processing technology. Another problem with focusing systems is that they cannot extract a „pure“ microbeam. For example, parabolic mirror neutron guides form beams strongly structured in space, refractive lenses focus only about 20–30% of the initial beam, and capillary lenses have a significant background. Calculations in Ref. [2] demonstrated that wings with the width from 10 to $20\,\mu$m remain when a microbeam with a width of about $100\,\mu$m is formed using a conventional diaphragm from blades of a neutron-absorbing crystal $Gd_3Ga_5O_{12}$ (or GGG). At the same time, the shape of the wings changes when the width of the diaphragm changes. A method for producing a microbeam with total specular reflection of neutrons from a silicon substrate is demonstrated in [2]. The method is suitable for time-of-flight technique, has a high intensity of the order of 1000 n/s and a low background of about 2 n/min, but the practically achieved width of the microbeam is still about $30\,\mu$m.

The narrowest microbeams of neutrons form three-layer waveguides (Figure 1). A collimated neutron beam with a width of about 0.1 mm and an angular divergence of about 0.01° falls at a small grazing angle α_s onto the surface of the waveguide in vacuum (medium 0). Then the neutrons tunnel through a thin upper layer with a thickness of 5–20 nm (medium 1) and fall into the middle layer with a thickness of d about 100–200 nm (medium 2). Next, the neutrons are almost completely reflected from the thick bottom layer with a thickness of 50–100 nm (medium 3) and then are partially reflected from the thin upper layer (medium 1). Part of the neutrons exits through the surface in the direction of the specularly reflected beam, and the other part of the neutrons propagates along the middle layer as in a channel (channelling) and exits from its end in the form of a narrow microbeam with a divergence $\delta\alpha_F$ of the order of 0.1°. The Fraunhofer diffraction makes the main contribution to the microbeam divergence on a narrow slit $\delta\alpha_F \propto \lambda/d$, where λ — the wavelength of neutrons. The initial width of the microbeam is d, and the final width is $w \approx d + l \cdot \delta\alpha_F$. Here l is the distance from the waveguide output. The investigated sample should be positioned as close as possible to the output end of the waveguide for maintaining the minimum width of the microbeam. The record narrow and „pure“ microbeam of neutrons are the advantages of layered waveguides, and the low intensity and relatively high angular divergence of the microbeam are the disadvantages of layered waveguides.

An unpolarized microbeam of neutrons from a three-layer waveguide was obtained in [3], and a polarized microbeam of neutrons was obtained in [4]. The contribution of Fraunhofer diffraction to the angular divergence of a

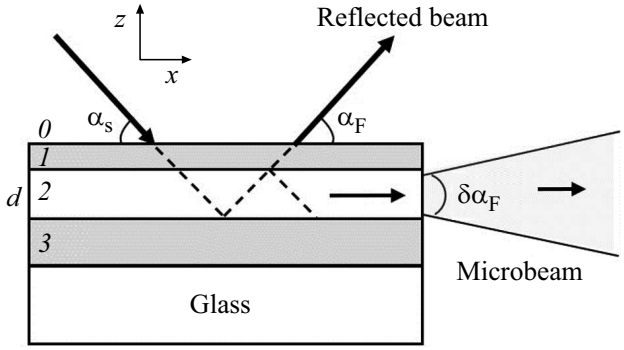

Figure 1. Geometry of the experiment with a microbeam of neutrons. The numbers indicate the indices of the medium where the neutrons enter: *0* — vacuum, *1* — upper magnetic layer, *2* — middle non-magnetic layer, *3* — lower magnetic layer.

microbeam was experimentally determined in in [5–7]. A neutron microbeam from a waveguide was used to study the magnetic microstructure in [8]. A magnetic wire with a diameter of 190 μm was scanned with a polarized microbeam with a width of 2.6 μm. A combination of a non-magnetic waveguide and a polarized neutron reflectometer was used in Ref. [9]. The experimental setup is described in more detail in Ref. [2]. It was demonstrated that statistically confident data can be obtained in a quite reasonable time of about 10 h at a microbeam intensity of the order of 1 n/s. It can be assumed that studies using neutron microbeads from waveguides will become more affordable with the introduction of new powerful neutron sources (ESS, PIK, IBR-3). Therefore, the study of the properties of neutron waveguides seems to be an actual task.

Two phenomena are simultaneously observed in the middle layer of the waveguide: the formation of resonantly enhanced neutron standing waves waves and channeling of neutrons. The theory of neutron resonances is described in Ref. [10] and the theory of channeling is described in Ref. [11]. Nanostructures are called resonators for practical reasons if resonant enhancement of the neutron wave field is used. If the phenomenon of neutron channeling is exploited in studies, then the same layered nanostructures are called waveguides.

Layered resonators are used to enhance the weak interaction of neutrons with the substance [12]. Neutron resonances manifest themselves as weak minima on the neutron specular reflection coefficients and as resonantly enhanced maxima of secondary characteristic radiation or specific neutron scattering corresponding to them. When neutrons interact with certain elements and isotopes, secondary characteristic radiation occurs as a result of nuclear reactions, for example, gamma quanta [13], alpha particles [14], products of the fission chain reaction [15]. An experimental setup with a polarized neutron reflectometer with simultaneous use of a gamma-ray detector is described in Ref. [16] and Ref. [17] describes an experimental setup with registration of alpha particles and tritons. The method of neutron reflectometry with registration of secondary characteristic radiation is described in detail in [18,19].

Neutrons that have experienced a spin flip during interaction with magnetically non-collinear layered structures [20–22], incoherently scattered on hydrogen [23], off-specularly scattered on the roughness of the interlayer boundaries [24,25] and on the domain structure can act as specific neutron scattering in the resonator [26,27]. Resonators were used in [28,29] to determine a small change of the concentration of hydrogen in a layered nanostructure.

The channeling of neutrons in layered waveguides is another type of specific neutron scattering. The phenomenon of channeling in the geometry of reflection was observed in [30], and neutron channeling was studied in detail in the geometry of a microbeam in [31–36]. It follows from the theory [11] that the square of the modulus of the neutron wave function exponentially decays inside the waveguide layer as $|\Psi|^2 \propto \exp(-x/x_e)$. Here x — the length of the path under the neutron absorber, which lies on the surface of the waveguide, and x_e — the length of channeling (the distance at which the neutron density attenuates in e times). The intensity of the neutron microbeam $I(x)$ from the end face of the waveguide is depending on the length of the absorber x is measured in the experiment described in [31] and then x_e is determined from the experimental dependence $I(x) = I(0)\exp(-x/x_e)$. Here $I(0)$ — the normalization intensity of the microbeam without an absorber. It is found that the length of neutron channeling is 1−5 mm. The channeling length decreases inversely with an increase of the resonance order of $n = 0, 1, 2, \ldots$ [33] and increases exponentially with an increase of the thickness of the upper layer [33], the thickness of the waveguide channel [34] and the depth of the quantum well of the waveguide [35]. The experimental setup is described in detail in Ref. [36]. The geometry of the microbeam makes it relatively easy to separate resonances from parasitic beams. The use of waveguides was proposed in Ref. [37] for a more accurate determination of the weak magnetization of a layer of the order of 100 G. This idea was experimentally implemented in Ref. [38.39]. The outer layers were non-magnetic in the three-layer waveguide and the studied ferrimagnetic films of $TbCo_5$ and $TbCo_{11}$ were used as the middle waveguide layer. The magnetization of the layer was directly determined by the position of the neutron energy resonances for spin „+“ and „–“. An overview of the studies and application of neutron waveguides is made in Ref. [40].

A waveguide in which the outer layers are magnetic, and uranium is placed in the middle non-magnetic layer was theoretically reviewed in Ref. [15]. It was proposed to change the gain of the neutron density inside the waveguide by remagnetization of the outer layers with a magnetic field. Such waveguides can be potentially applied for fission chain reaction control in a miniature nuclear power plant. We consider similar waveguides with external magnetic layers in this paper.

2. Calculations

Calculations were made according to the theory of neutron resonances in the layered nanostructures [10]. Let us introduce the following notations:

$$k_{0z} = \frac{2\pi}{\lambda}\sin\alpha_s,\ k_{1z} = \sqrt{k_{0z}^2 - \rho_1},\ k_{2z} = \sqrt{k_{0z}^2 - \rho_2},$$

$$k_{0x} = \frac{2\pi}{\lambda}\cos\alpha_s.$$

Here ρ_1 — neutron scattering length density (SLD) for the upper layer 1, ρ_2 — SLD for the waveguide layer 2. The neutron wave function has the general form of $\Psi(k_{0z}, z) = A\exp(ik_{0z}z)$, where A — the amplitude of the wave function. Then we obtain that $|\Psi|^2 = |A|^2$. The wave function has the form inside the middle layer

$$\Psi(k_{0z}, z) = A[\exp(-ik_{2z}z) + r_{23}\exp(ik_{2z}z)],$$

where r_{23} — the amplitude of reflection of the neutron wave function from the lower layer 3. The amplitude A is determined from the self-consistent equation for the neutron wave function in the layer 2 if the origin of the coordinates $z = 0$ is combined with the interface of layers 1 and 2:

$$A = t_{02}\exp(ik_{2z}d) + r_{21}r_{23}\exp(ik_{2z}2d)A, \qquad (1)$$

where t_{02} — the amplitude of transmission of the neutron wave function from vacuum to medium 2 through layer 1, r_{21} — the amplitude of reflection of the neutron wave function in the medium 2 from layer 1. The following is found from a self-consistent equation (1)

$$|\Psi|^2 = |A|^2 = \frac{|t_{02}|}{|1 - r_{21}r_{23}\exp(2ik_{2z}d)|}. \qquad (2)$$

The value $|\Psi|^2 = |A|^2$ in the equation (2) has resonant maxima under periodic conditions for the phase of the neutron wave function

$$\Phi(k_{0z}) = 2k_{2z}d + \arg(r_{21}) + \arg(r_{23}) = 2\pi n, \qquad (3)$$

where $n = 0, 1, 2, \ldots$ is the resonance order. If the neutron wavelength is fixed, the grazing angle of the initial beam has resonances along the angle α_{sn}. If the time-of-flight method is used, then the grazing angle of the initial beam is fixed, and the final neutron spectrum has resonances along the wavelength λ_n.

Let us consider two waveguides:

Py(20 nm)|Cu(140 nm)|Py(50 nm) || glass

and Fe(20 nm)|Cu(140 nm)|Fe(50 nm) || glass.

Permalloy (Py) is a magnetic alloy of Fe (20.6 at.%)-Ni (79.4 at.%) with a narrow hysteresis loop and saturation magnetization of about 10 kG. Figure 2 shows the SLD of waveguides depending on the coordinate z in the direction perpendicular to the layers. The tabular values of the nuclear part of the SLD are taken for calculations. The magnetization of the Fe layers is equal to the saturation

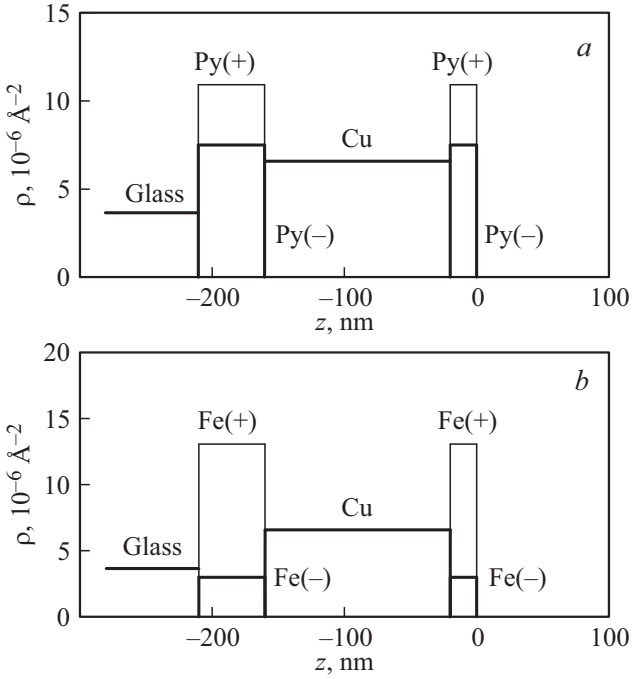

Figure 2. Scattering length density (SLD) of neutrons of a waveguide with external magnetic layers for neutron polarization „+“ and „–“: *a* — Py(20 nm)|Cu(140)|Py(50) || glass; *b* — Fe(20 nm)|Cu(140)|Fe(50) || glass.

magnetization of 22.0 kG. The saturation magnetization of 7.2 kG is assumed for permalloy. The SLD of the outer layers is equal to $\rho_1 = \rho_{1N} \pm \rho_{1M}$, where ρ_{1N} — contribution of the nuclear interaction of neutrons with matter, $\rho_{1M} \propto M$ — contribution of the magnetic interaction of neutrons with matter, M — the magnetization of the layers. The signs „+“ and „–“ correspond to the sign of the projection of the neutron spin on the direction of magnetization of the layers. The wavelength of neutrons is 4.26 Å, the wavelength resolution is 0.05 Å, the grazing angle resolution of the initial beam is 0.006°. It can be seen that the SLD for neutrons with spin „+“ has the form of a deep well for both waveguides. The SLD for the Py|Cu|Py waveguide has the form of a shallow pit for neutrons with spin „–“ (Figure 2, *a*) and it has the form of a low barrier for the Fe|Cu|Fe waveguide (Figure 2, *b*).

Figure 3 shows the square of the modulus of the neutron wave function depending on the grazing angle of the incident neutron beam with spin „+“ (up) and „–“ (do or down), summed along the coordinate z inside the waveguide layer. The indices $n = 0, 1, 2, \ldots$ indicate the orders of resonances. It can be seen that the gain is 30 for spin up and 15 for spin do for the Py|Cu|Py waveguide (Figure 3, *a*) in resonance $n = 0$. The positions of resonance $n = 0$ for the up and do spins practically coincide with each other, which is determined by the magnitude of the SLD of the Cu waveguide layer. The positions of higher-order resonances $n = 1, 2, \ldots$ for the do spin are shifted to smaller angles relative to the resonances for the up spin. The neutron

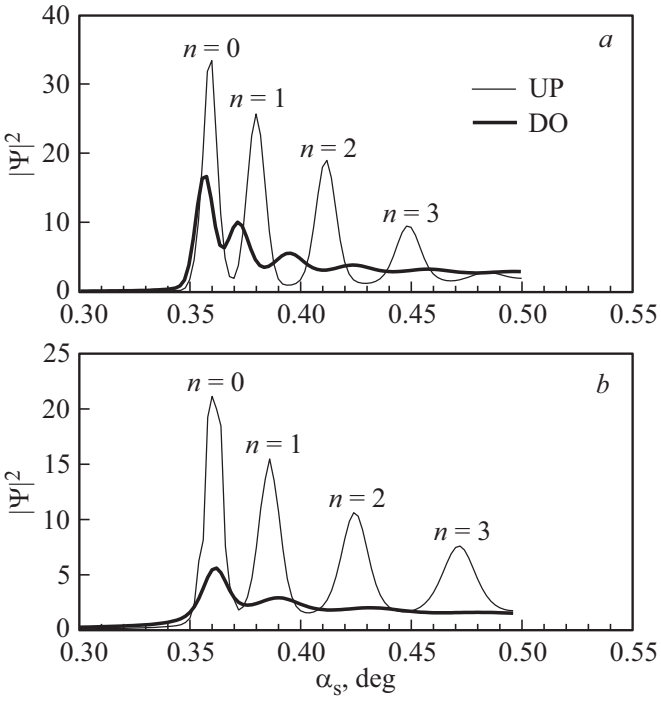

Figure 3. Calculation of the square of the modulus of the neutron wave function inside the waveguide depending on the grazing angle of the incident beam with polarization UP (thin line) and DO (thick line): *a* — Py|Cu|Py; *b* — Fe|Cu|Fe.

density gain in resonance $n = 0$ is 20 for spin up and 5 for spin do in case of the Fe|Cu|Fe waveguide (Figure 3, *b*). The positions of resonance $n = 0$ for the up and do spins also practically coincide with each other, as well as for the Py|Cu|Py waveguide. At the same time, the maximum resonances of higher orders ($n = 1, 2$) are weakly expressed.

Therefore, the calculations have shown that the neutron density gain in resonance of the order $n = 0$ is much higher for the up spin than for the do spin. The ratio of the neutron density gain coefficients for the up and do spin is 2 for the Py|Cu|Py waveguide and 4 for Fe|Cu|Fe waveguide. Next, let's look at the experimental results.

3. Experimental results

The experiments were performed using polarized neutron reflectometer NREX [41]. A neutron beam with a wavelength of 4.26 Å and a degree of polarization of 0.97 was used. A single supermirror in the transmission geometry was used as a polarizer. The direction of polarization of the neutron beam in front of the sample was changed using a Mesey spin-flipper. The sample sizes are $30 \times 30 \times 5$ mm. The divergence of the incident beam is 0.006°, the neutron wavelength resolution is 1.0%. An external magnetic field is applied parallel to the sample plane to magnetize the film to saturation. The strength of the applied magnetic field was 1.0 kOe for the Py|Cu|Py waveguide and 1.5 kOe for Fe|Cu|Fe waveguide. The angular resolution of the ^{3}He gas two-dimensional position-sensitive detector (PSD) is 0.072°. The distance from the first 0.25 mm wide diaphragm to the sample was 2200 mm, and the distance from the sample to the detector was 2400 mm. The spatial resolution of the detector is 3.0 mm. There was a second diaphragm with a width of 0.7 mm in front of the sample at a distance of 200 mm, the purpose of this aperture was to reduce the background.

The neutron specular reflection coefficients for up and do beam polarization were measured to characterize the waveguide structure (Figure 4). Figure 4, *a* shows the coefficients of specular reflection from the Py|Cu|Py waveguide. The symbols correspond to the experiment, the lines correspond to the results of fitting of the computed model of the structure to the experimental data. The following waveguide parameters were obtained

$$\text{PyO}(2.3\,\text{nm}, 7.67 \cdot 10^{-6}\,\text{Å}^{-2})|\text{Py}(19.5, 8.83 \cdot 10^{-6},$$

$$7.0\,\text{kG})|\text{Cu}(132.0, 6.58 \cdot 10^{-6})|\text{Py}(48.0, 8.56 \cdot 10^{-6},$$

$$7.2\,\text{kG})||\text{glass}(2.63 \cdot 10^{-6}\,\text{Å}^{-2}).$$

The thicknesses of the layers in [nm], the nuclear part of the SLD in [Å^{-2}] and the magnetization in [kG] are specified here. The magnetization of the upper thin permalloy layer is 7.0 kG, and the lower thick layer has a magnetization of 7.2 kG as a result of the fitting. The top layer has a thin non-magnetic PyO film as a result of oxidation. The oxidation process is a conventional process,

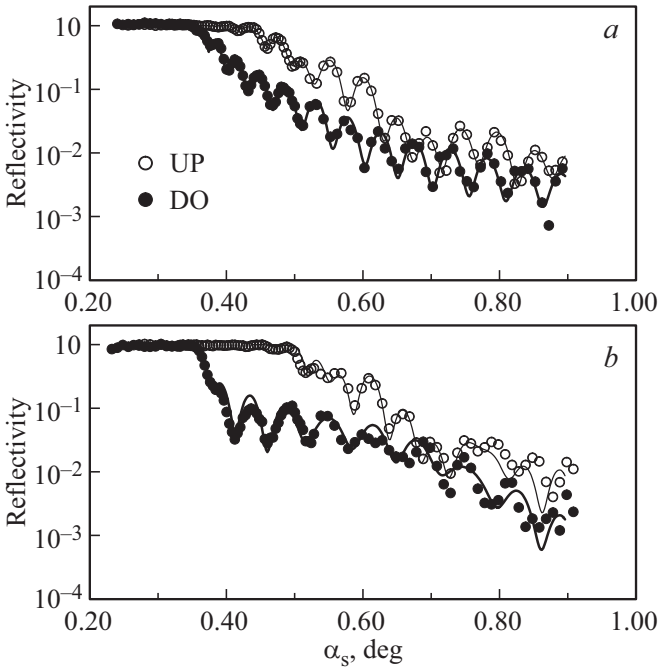

Figure 4. Neutron specular reflection coefficients for polarization of the incident beam UP (open symbols) and DO (closed symbols): *a* — Py|Cu|Py; *b* — Fe|Cu|Fe. Dots — the experiment, lines — fitting.

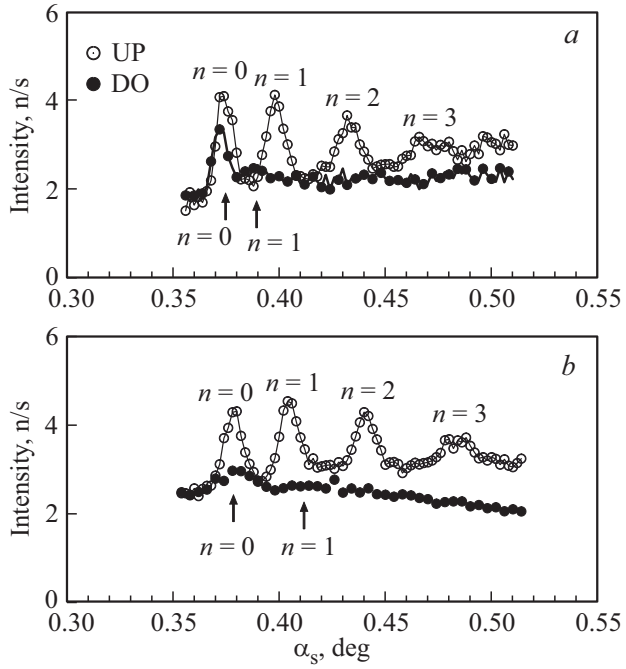

Figure 5. Neutron microbeam intensity for polarization of the incident beam UP (open symbols) and DO (closed symbols): *a* — Py|Cu|Py; *b* — Fe|Cu|Fe.

unless special actions are taken. For example, sputtering of a protective layer on the surface of the film.

Figure 4, *b* shows the coefficients of neutron specular reflection from the Fe|Cu|Fe waveguide (symbols — experiment, lines — fitting). The following parameters are obtained as a result of the fitting

$$\mathrm{FeO}(5.4\,\mathrm{nm},\ 7.49\cdot 10^{-6}\,\mathrm{\AA}^{-2})$$

$$|\mathrm{Fe}(15.4\,\mathrm{nm},\ 8.03\cdot 10^{-6}\,\mathrm{\AA}^{-2},\ 22.0\,\mathrm{kG})|$$

$$\mathrm{Cu}(136.0\,\mathrm{nm},\ 6.96\cdot 10^{-6}\,\mathrm{\AA}^{-2})$$

$$|\mathrm{Fe}(51.0\,\mathrm{nm},\ 8.03\cdot 10^{-6}\,\mathrm{\AA}^{-2},\ 22.0\,\mathrm{kG})|$$

$$|\mathrm{glass}(3.97\cdot 10^{-6}\,\mathrm{\AA}^{-2}).$$

It can be noted that the oxide layer for iron is larger than for permalloy. The magnetization of iron saturation is equal to the tabular value.

Next, the intensity of the neutron microbeam depending on the grazing angle of the incident polarized beam was measured in the experiment (Figure 5). Figure 5, *a* shows the intensity of the neutron microbeam for the Py|Cu|Py waveguide. The magnitude of the intensity statistical error is equal to the size of the symbols and less. It can be seen that the background level in the resonance region $n = 0$ is 2.1 n/s. The intensity of the microbeam in resonance $n = 0$ after substraction of the background equals to 2.0 n/s for the polarization of the incident beam up and 1.2 n/s for the polarization do. Then the ratio of the microbeam intensities for up and do polarization is 1.7 ± 0.3. It is important to note here that it was possible to significantly reduce the background in the microbeam in the experiment with the microwire [2,8]. A Cd plate was glued to the input end face of the waveguide substrate for this purpose and a blade made of a neutron-absorbing GGG crystal was placed on the surface of the waveguide near the outlet. The background was about 10 times less than the useful signal as a result. Such a strong reduction of the background was not a task of this experiment. A simple design of two Cd plates was used at a distance of approximately 700 mm from the sample position for blocking the direct and reflected beams: a plate on a rack with a stepper motor, which blocked the direct beam, and a plate on a moving massive protection of the PSD, which blocked the reflected beam.

The background level in the region of resonance $n = 0$ is 2.4 n/s for the Fe|Cu|Fe waveguide (Figure 5, *b*). The intensity of the microbeam in the resonance $n = 0$ after substraction of the background is 1.9 n/s for the polarization of the incident beam up and 0.5 n/s for the polarization do. The ratio of the microbeam intensities for up and do polarization is 3.8 ± 0.5 as a result. It can be noted that the intensity of the neutron microbeam for up polarization is significantly higher than for do polarization for both waveguides. Therefore, the obtained experimental data confirm the preliminary calculations based on the theory of resonances.

4. Discussion of the results

Neutron waveguides consisting of external magnetic layers and a non-magnetic middle layer are studied in this paper. A polarized initial neutron beam and films magnetized to saturation were used. The SLD of the outer layers changes, while the SLD of the middle layer remains constant. The position of the resonances for the initial polarization of up and do slightly varies in such a resonant structure and the gain of the neutron density varies greatly. The wavelength of the neutrons was fixed. The intensity of a microbeam of neutrons coming out of the end face of a non-magnetic waveguide layer was measured. It is found that the intensity of the microbeam in the resonance of the order $n = 0$ for up polarization is several times higher than for do polarization. This ratio is even higher for resonances of higher orders. Therefore, it was experimentally demonstrated that the magnetic structure of the waveguide affects the magnitude of the neutron density gain inside the waveguide. The state of the magnetic film does not change in this case, but the polarization of the beam incident on the sample changes.

It is possible to change the gain of the neutron density in another way. For example, it is possible to use an initial beam with a fixed up polarization and remagnetize the magnetic layers using an applied time-oscillating magnetic

field. The method of neutron reflectometry in an alternating magnetic field and an experimental setup are described in Ref. [42,43]. The method is used to study the dynamics of the domain structure in films. The switching frequency of the magnetic field is about 300 kHz. In this case, the frequency and amplitude of the alternating magnetic field can be changed, as well as the time ratio for positive and negative magnetization of the film. This method is more complex, but it gives more opportunities to influence the state of the sample and the gain factor of the neutron density. It will be necessary to study possible depolarization processes of a neutron beam in interaction with a waveguide in this case.

The advantage of a waveguide with external magnetic layers and a middle non-magnetic layer is as follows. If the time-of-flight technique is used, then at a fixed grazing angle of the incident neutron beam, all neutrons with a set of wavelengths λ_n in resonances $n = 0, 1, 2, \ldots$ are present in the microbeam spectrum, while the intensity of the microbeam of neutrons with do polarization in resonances is small compared with up polarization (Figure 5, *b*). If we take, for example, a Fe|Co|Fe waveguide with three magnetic layers [44], then the position of the resonances for do polarization will be strongly shifted along the neutron wavelength. But neutrons with do polarization in resonances will be still present in the spectrum. Approximately the same happens in waveguides with non-magnetic outer layers and a magnetic middle layer [38–40,45]. The position of the neutron resonances is split in energy to polarize up and do, but the amplitudes of the resonances remain approximately the same. Therefore, neutrons with opposite polarization will be present in the time-of-flight spectrum of the microbeam.

The principle of operation of a waveguide with external magnetic layers is considered in the most general form in this paper. It is shown that the amplitude of the intensity of the microbeam in resonances for the initial polarization of up is significantly higher than the intensity for the polarization of do. The calculations did not taken into consideration the dependence of the amplitude and width of neutron resonances on the parameters of the structure and experimental conditions. The width of neutron resonances in a non-magnetic waveguide was theoretically and experimentally studied in [46] as a function of the angular divergence of the incident neutron beam. It was found that the spectral width of neutron resonances increases with an increase of the angular divergence of the incident neutron beam. An experimental estimate of the intrinsic width of neutron resonances in a waveguide was obtained in the same paper. It follows from these results that in the future it is necessary to conduct additional studies of the effect of the processes of remagnetization of the external magnetic layers of the waveguide on the amplitude and width of neutron resonances.

5. Conclusion

Neutron waveguides Py|Cu|Py and Fe|Cu|Fe with external magnetic layers and a non-magnetic middle layer were studied. Calculations based on the theory of resonances in layered structures demonstrated that the gain coefficient of the neutron density in such waveguides in resonances for the initial beam polarization up is significantly higher than for polarization do. A collimated polarized neutron beam was incident on the surface of a magnetic waveguide in this experiment. Then the neutrons were channeled along the middle non-magnetic layer and exited from the end face of the channel in the form of a diverging beam of micron width. The intensity of the neutron microbeam was registered depending on the polarization sign of the incident neutron beam. It was found that the intensity of the microbeam of neutrons in resonance of the order $n = 0$ for do polarization is less than the intensity of the microbeam for up polarization in 1.7 ± 0.3 times for the Py|Cu|Py waveguide and in 3.8 ± 0.5 times for the Fe|Cu waveguide|Fe. The experimental data confirm the preliminary calculations. Waveguides of this type can be potentially applied for controlling the chain reaction of uranium fission using an external magnetic field to create a miniature nuclear power plant [15].

Acknowledgments

The authors thank A. Rühm for assistance in conducting experiments on the neutron reflectometer NREX.

Conflict of interest

The authors declare that they have no conflict of interest.

References

[1] F. Ott. Focusing Optics for Neutrons. In: Modern Developments in X-Ray and Neutron Optics. Springer Series in Optical Sciences. (2008). V. 137. P. 113–134.
[2] F. Ott, S. Kozhevnikov, A. Thiaville, J. Torrejón, M. Vázquez. Nucl. Instrum. Meth. A **788**, 29 (2015).
[3] F. Pfeiffer, V. Leiner, P. Høghøj, I. Anderson. Phys. Rev. Lett. **88**, *5*, 055507 (2002).
[4] S.V. Kozhevnikov, A. Rühm, F. Ott, N.K. Pleshanov, J. Major. Physica B **406**, *12*, 2463 (2011).
[5] S.V. Kozhevnikov, V.K. Ignatovich, Yu.V. Nikitenko, F. Ott, A.V. Petrenko. JETP Lett. **102**, *1*, 1 (2015).
[6] S.V. Kozhevnikov, V.D. Zhaketov, F. Radu. JETP **127**, *4*, 593 (2018).
[7] S.V. Kozhevnikov, V.D. Zhaketov, T. Keller, Yu.N. Khaydukov, F. Ott, F. Radu. Nucl. Instrum. Meth. A **915**, 54 (2019).
[8] S.V. Kozhevnikov, F. Ott, J. Torrejón, M. Vázquez, A. Thiaville. Phys. Solid State **56**, *1*, 57 (2014).
[9] S.V. Kozhevnikov, A. Rühm, J. Major. Crystallogr. Rep. **56**, *7*, 1207 (2011).
[10] F. Radu, V.K. Ignatovich. Physica B **292**, *1–2*, 160 (2000).
[11] V.K. Ignatovich, F. Radu. Phys. Rev. B **64**, *20*, 205408 (2001).
[12] Yu.V. Nikitenko. Phys. Particles Nuclei **40**, *6*, 890 (2009).

[13] H. Zhang, P.D. Gallagher, S.K. Satija, R.M. Lindstrom, R.L. Paul, T.P. Russell, P. Lambooy, E.J. Kramer. Phys. Rev. Lett. **72**, *19*, 3044 (1994).
[14] V.L. Aksenov, Yu.V. Nikitenko, F. Radu, Yu.M. Gledenov, P.V. Sedyshev. Physica B **276**–**278**, 946 (2000).
[15] S.P. Pogossian. J. Appl. Phys. **102**, *10*, 104501 (2007).
[16] V.D. Zhaketov, K. Hramco, A.V. Petrenko, Yu.N. Khaydukov, A. Csik, Yu.N. Kopatch, N.A. Gundorin, Yu.V. Nikitenko, V.L. Aksenov. J. Surface Investigation: X-ray, Synchrotron. Neutron Techniques **15**, *3*, 549 (2021).
[17] V.D. Zhaketov, A.V. Petrenko, S.N. Vdovichev, V.V. Travkin, A. Csik, Yu.N. Kopatch, Yu.M. Gledenov, E. Sansarbayar, N.A. Gundorin, Yu.V. Nikitenko, V.L. Aksenov. J. Surface Investigation: X-ray, Synchrotron. Neutron Techniques **13**, *3*, 478 (2019).
[18] Yu.V. Nikitenko, A.V. Petrenko, N.A. Gundorin, Yu.M. Gledenov, V.L. Aksenov. Crystallogr. Rep. **60**, *4*, 466 (2015).
[19] V.L. Aksenov, V.D. Zhaketov, Yu.V. Nikitenko. Phys. Particles. Nuclei **54**, *4*, 756 (2023).
[20] V.L. Aksenov, Yu.V. Nikitenko, S.V. Kozhevnikov, F. Radu, R. Kruijs, T. Rekveldt. J. Surface Investigation: X-ray, Synchrotron. Neutron Techniques **16**, *8*, 1225 (2001).
[21] Yu. Khaydukov, A.M. Petrzhik, I.V. Borisenko, A. Kalabukhov, D. Winkler, T. Keller, G.A. Ovsyannikov, B. Keimer. Phys. Rev. B **96**, *16*, 165414 (2017).
[22] Yu.N. Khaydukov, D. Lenk, V. Zdravkov, R. Morari, T. Keller, A.S. Sidorenko, L.R. Tagirov, R. Tidecks, S. Horn, B. Keimer. Phys. Rev. B **104**, *17*, 174445 (2021).
[23] M. Wolff, A. Devishvili, J.A. Dura, F.A. Adlmann, B. Kitchen, G.K. Pálsson, H. Palonen, B.B. Maranville, Ch.F. Majkrzak, B.P. Toperverg. Phys. Rev. Lett. **123**, *1*, 016101 (2019).
[24] S.V. Kozhevnikov, F. Ott, E. Kentzinger, A. Paul. Physica B **397**, *1*–*2*, 68 (2007).
[25] S.V. Kozhevnikov, F. Ott, A. Paul, L. Rosta. Eur. Phys. J. Spec. Topics **167**, *1*, 87 (2009).
[26] E. Kentzinger, U. Rücker, B. Toperverg, T. Brückel. Physica B **335**, *1*–*4*, 89 (2003).
[27] F. Radu, A. Vorobiev, J. Major, H. Humblot, K. Westerholt, H. Zabel. Physica B **335**, *1*–*4*, 63 (2003).
[28] L. Guasco, Yu.N. Khaydukov, S. Pütter, L. Silvi, M.A. Paulin, T. Keller, B. Keimer. Nature Commun. **13**, *1*, 1486 (2022).
[29] A. Perrichon, A. Devishvili, K. Komander, G.K. Pálsson, A. Vorobiev, R. Lavén, M. Karlsson, M. Wolff. Phys. Rev. B **103**, *23*, 235423 (2021).
[30] V.L. Aksenov, Yu.V. Nikitenko. Physica B **297**, *1*–*4*, 101 (2001).
[31] S.V. Kozhevnikov, V.K. Ignatovich, F. Ott, A. Rühm, J. Major. JETP **117**, *4*, 636 (2013).
[32] Yu.V. Nikitenko, V.V. Proglyado, V.L. Aksenov. J. Surface Investigation. X-ray, Synchrotron. Neutron Techniques **8**, *5*, 961 (2014).
[33] S.V. Kozhevnikov, V.D. Zhaketov, Yu.N. Khaydukov, F. Ott, F. Radu. JETP **125**, *6*, 1015 (2017).
[34] S.V. Kozhevnikov, T. Keller, Yu.N. Khaydukov, F. Ott, F. Radu. JETP **128**, *4*, 504 (2019).
[35] S.V. Kozhevnikov, Yu.N. Khaydukov, F. Ott, F. Radu. JETP **126**, *5*, 592 (2018).
[36] S.V. Kozhevnikov, T. Keller, Yu.N. Khaydukov, F. Ott, F. Radu. Nucl. Instrum. Meth. A **875**, 177 (2017).
[37] S.P. Pogossian, H. Le Gall, A. Menelle. J. Magn. Magn. Mater. **152**, *3*, 305 (1996).
[38] S.V. Kozhevnikov, Yu.N. Khaydukov, T. Keller, F. Ott, F. Radu. JETP Lett. **103**, *1*, 36 (2016).
[39] S.V. Kozhevnikov, V.D. Zhaketov, T. Keller, Yu.N. Khaydukov, F. Ott, Chen Luo, Kai Chen, F. Radu. Nucl. Instrum. Meth. A **927**, 87 (2019).
[40] S.V. Kozhevnikov. Phys. Particl. Nucl. **50**, *3*, 300 (2019).
[41] Yu.N. Khaydukov, O. Soltwedel, T. Keller. J. Large Scale Res. Facilities **1**, A38 (2015).
[42] K. Zhernenkov, S. Klimko, B.P. Toperverg, H. Zabel. J. Physics: Conf. Ser. **211**, 012016 (2010).
[43] S. Klimko, K. Zhernenkov, B.P. Toperverg, H. Zabel. Rev. Scientific Instrum. **81**, *10*, 103303 (2010).
[44] S. Kozhevnikov, T. Keller, Yu. Khaydukov, F. Ott, A. Rühm, J. Major. Phys. Procedia **42**, 80 (2013).
[45] A. Rühm, S.V. Kozhevnikov, F. Ott, F. Radu, J. Major. Nucl. Instrum. Meth. A **708**, 83 (2013).
[46] S.V. Kozhevnikov, V.K. Ignatovich, A.V. Petrenko, F. Radu. JETP **123**, *6*, 950 (2016).

Translated by A.Akhtyamov